Geoderma 440 (2023) 116718

Contents lists available at ScienceDirect

Geoderma

journal homepage: www.elsevier.com/locate/geoderma

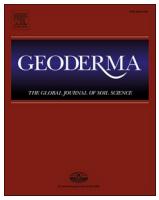

Metal cation concentrations improve understanding of controls on soil organic carbon across a precipitation by vegetation gradient in the Patagonian Andes

Caitlin Hodges [a,*], Patricia I. Araujo [b,c], Laura J.T. Hess [b], Lucía Vivanco [b], Jason Kaye [d], Amy T. Austin [b]

[a] University of Oklahoma, School of Geosciences, 100 E Boyd St, 710 Sarkeys Energy Center, Norman, OK 73019
[b] Instituto de Investigaciones Fisiológicas y Ecológicas Vinculadas a la Agricultura (IFEVA), Consejo Nacional de Investigaciones Científicas y Técnicas (CONICET), Facultad de Agronomía, Universidad de Buenos Aires, Av. San Martín 4453, Buenos Aires, Argentina
[c] Estación Experimental Agropecuaria Pergamino, Instituto Nacional de Tecnología Agropecuaria (INTA), Ruta 32 km 4.5, 2700 Pergamino, Buenos Aires, Argentina
[d] The Pennsylvania State University, Department of Ecosystem Science and Management, University Park, Pennsylvania

ARTICLE INFO

Handling editor: Cornelia Rumpel
Handling Editor: C. Rumpel

Keywords:
Andisol
Tephra
Afforestation
Carbon dioxide removal
Mineral associated organic matter
Cation bridging

ABSTRACT

Tephra-derived soils retain more organic carbon (C) than soils formed from any other parent material, but this C may be sensitive to changes in climate and land use. Here we evaluate the effects of precipitation, temperature, and afforestation on extractable metals and organic C storage in young tephra-derived soils in a temperate climate. We conducted our investigation across five sites in the Patagonian Andes that vary from 250 mm to 2200 mm mean annual precipitation, and 12 to 9.7 ℃ mean annual temperature from east to west. At each of the five sites are paired plots of natural vegetation, varying from grasses and shrubs at the dry sites to closed-canopy forest at the wet, and stands of *Pinus ponderosa* planted in monocultures 35 years prior to sampling. Previous research at these sites showed that aboveground net primary production and soil organic C increased with rainfall, but total soil organic C content was lower in pine plantations than natural vegetation. Here we assess whether variation in precipitation and vegetation type also affect soil mineral properties that promote soil C stabilization. Soils were collected to the depth of auger refusal and extracted with 0.5 M HCl for 24 h to target the combined exchangeable and adsorbed metals, including secondary short-range-ordered mineral phases and the plant available pools of Mg, Ca, and K. Pine afforestation lowered concentrations of HCl-extractable K ($p < 0.1$) and Ca ($p < 0.01$) within the top 0 – 30 cm. Other elements, while not affected by vegetation type, did respond to the rainfall gradient. Al, Si, P, and Mn all increased in the surface soils with increasing rainfall ($p < 0.01$), suggesting the development of short-range-order volcanic mineral phases that retain nutrients such as P and Mn. The addition of Al and Ca in the linear model to describe soil organic C explained more of the total variance than rainfall and vegetation type alone, indicating the importance of Al complexes and cation (Ca) bridging with secondary minerals to soil C retention. Importantly, the lower concentration of Ca in planted pine soils may signal a long-term decrease in the potential soil C stored in afforested soils due to a lower capacity for cation bridging. Our results show that the chemistry of these young tephra soils is dynamic, responding to both precipitation and afforestation in distinct ways with potential long-term impacts on nutrient cycling and C storage.

1. Introduction

Soils represent the largest terrestrial pool of organic carbon (OC), and therefore are key to regulation of the global C cycle (Amundson, 2001). In general, the amount of OC in soils is determined by the balance between inputs of plant and microbial biomass and microbial decomposition of those inputs (Chapin et al. 2011). Climate, plant litter quality, and soil mineralogy have been identified as key factors that determine differences in soil OC stocks across sites, and over the course of soil development, the key mechanisms of soil C retention shift (Mikutta et al., 2009; Doetterl et al., 2015; Lawrence et al., 2021). In base-rich soils with neutral to slightly acidic pH, aluminosilicates retain

* Corresponding author.
E-mail address: chodges@ou.edu (C. Hodges).

https://doi.org/10.1016/j.geoderma.2023.116718
Received 11 May 2023; Received in revised form 3 November 2023; Accepted 13 November 2023
Available online 22 November 2023

soil organic carbon (SOC) through cation bridging with multi-valent cations such as Ca and Mg (Rowley et al., 2018). As soils weather and lose base cations, most soil OC stabilization occurs by direct sorption onto high surface area, short-range-order (SRO) minerals, and coprecipitation with Fe and Al (Rasmussen et al., 2005; Mikutta et al., 2006; Kleber et al., 2015). Following this pattern, in young soils derived from volcanic tephra, most soil C is co-precipitated with metals, complexed with Al and Fe, or adsorbed, either directly or through cation bridging, to reactive mineral surfaces (Chorover et al., 2004; Matus et al., 2014; Kramer and Chadwick, 2016). Because this mineral and metal associated OC is considered the more stable pool of C in soils, the factors governing the retention of OC in mineral associations are important to identify within and across ecosystems.

The interaction between SOC and soil development has been explored for decades, but conflicting results reveal that no broadly applicable model of soil C storage can be applied across sites globally. For example, soil texture, soil Ca, soil Al, plant litter quality, and soil order have all been found to be the "most important' factor governing SOC retention in various studies (Matus et al., 2006; Garrido and Matus, 2012; Mathieu et al., 2015; Blankinship et al., 2018; Harden et al., 2018; Rasmussen et al., 2018). While there is no consensus in the literature on the key factors controlling SOC retention, the current body of work does indicate that soil mineral composition and vegetation type significantly affect soil C storage.

These key controls on the retention of SOC may also be affected by additional factors including land-use and climate change. One change in land-use that had been proposed for lowering atmospheric CO_2 levels is afforestation of grasslands and previously forested landscapes (Jandl et al., 2007; Nave et al., 2018). The increased aboveground net primary production (ANPP) of ecosystems planted with young, fast-growing trees is intended as a sink for anthropogenic CO_2 emissions. However, the effects of such afforestation on soil development and SOC dynamics in naturally unforested areas are underexplored. Understanding the changes in soil development and SOC caused by afforestation initiatives is imperative to accurately assess the viability and consequences of such projects.

Because tephra-derived soils represent a terrestrial C pool disproportionately high relative to their global distribution (Matus et al., 2014; Kramer and Chadwick, 2016; Ugolini and Dahlgren, 2002), we sought to identify how the factors that affect the retention of OC in volcanic soils in natural and afforested ecosystems may shift across a precipitation gradient in the Patagonian Andes of Argentina. This precipitation gradient (Fig. 1), established by Araujo (2012) and Hess & Austin (2014), presents an ideal arena for our research goals. The gradient is comprised of five sites that range from 250 mm to 2200 mm of mean annual precipitation (MAP) from east to west. Mean annual temperature (MAT) of the sites is well-constrained and varies from 8.9 °C at the 1100 mm MAP site and 12 °C at the 250 mm MAP site. At each of the five precipitation levels along the gradient is a naturally vegetated plot and a planted exotic *Pinus ponderosa* plantation plot. The pines across the gradient were all planted in the late 1970 s with minimal subsequent management (Araujo and Austin, 2015).

We hypothesized that base cation concentrations would be lower in soils afforested with *Pinus ponderosa* when compared to the naturally vegetated soils. In general, conifers have nutrient conservation strategies such as long leaf lifespan, low leaf tissue nutrient concentration, and slow decomposition rates, when compared to grasses, broadleaf woody trees, and shrubs (Jobbágy and Jackson 2003). Therefore, the faster decomposing litter of grass, broadleaf woody trees and shrubs, and herbaceous plants replenishes nutrient supply, especially base cations, to soils at a faster rate than conifers, which results in higher base cation concentrations in soils (Jobbágy and Jackson 2003; Berthrong et al. 2009; Schaetzl & Thompson, 2015). Second, we hypothesized that inclusion of geogenic metal concentrations from soil extractions in a multivariate model of SOC would improve explained variance of SOC concentrations across the rainfall gradient. Prior work across the

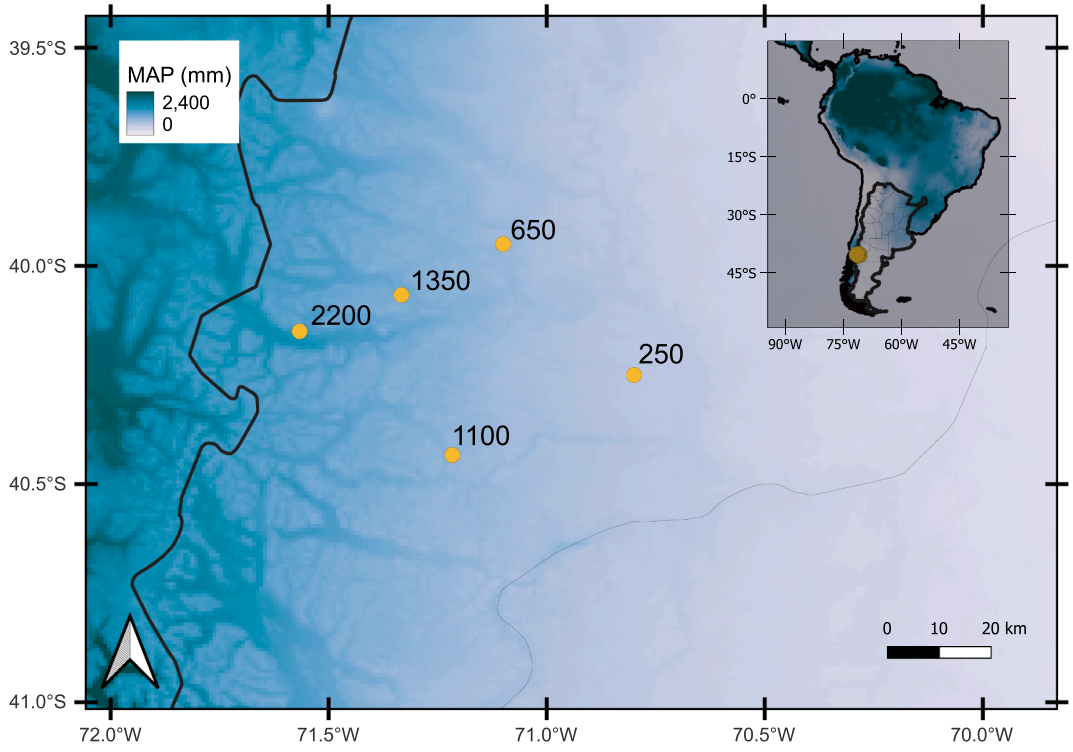

Fig. 1. Map of study sites in northwest Patagonia, Argentina. Yellow symbols represent the locations of each paired natural vegetation and pine plantation site and adjacent text is the long-term mean annual precipitation (MAP) in mm. The color gradient of the map indicates MAP in each zone, with darker green indicated higher MAP and light blue to more arid zones. More details about the sites and locations can be found in Araujo and Austin, (2015, 2020). (For interpretation of the references to color in this figure legend, the reader is referred to the web version of this article.)

gradient showed that SOC concentrations correlate strongly with MAP, but that planted pine soils are also overall lower in SOC (Hess and Austin, 2014). With inclusion of metal cations in our analysis, we sought to account for more of the variance in SOC concentrations, and potentially explain differences in SOC between native and afforested soils.

To address our hypotheses, we extracted soils collected from the naturally vegetated and afforested sites at common depth increments. The extraction we used targets the amorphous phases of Fe and Al oxyhydroxides, and the exchangeable or adsorbed metals associated with these phases. We first assessed the effects of vegetation type, MAP, and mean annual temperature on extracted metals concentrations. Then, we evaluated the effect of plant biomass production on metal concentrations, after accounting for the variance in the data explained by vegetation type and MAP. We used this analysis to determine whether SOC concentration is different between the afforested and natural vegetation sites simply because there are differences in primary productivity (carbon fixation), or whether mineral-controlled soil C storage mechanisms also affect SOC concentrations. Finally, we augmented prior models of SOC across our research sites with the extracted metal concentrations to establish whether changes in soil organic matter pools were correlated with soil mineral composition. This work elucidates both the shifting role of minerals in soil C retention and the potential effects of afforestation on the stability of the belowground C pool.

2. Materials and methods

2.1. Site description

Soils were sampled from sites established by Araujo (2012) and Hess and Austin (2014), distributed across a precipitation gradient in the northwest of the Patagonian region in Argentina, in the Neuquén province (Fig. 1). The sites, each with paired sub-sites in natural vegetation and *Pinus ponderosa* stands planted 1974—1976, are located along a 60 km east–west transect that vary in long-term MAP from 250 to 2200 mm (Araujo and Austin 2020). Precipitation is strongly seasonal and mostly falls between May and September (Southern Hemisphere winter). The MAT of the five sites does not covary with MAP; MAT is maximum 12 °C at the 250 mm MAP site, 9.5 °C at 650 mm MAP, minimum at 8.9 °C at 1100 mm MAP, 11 °C at 1350 mm MAP, and 9.7 °C at 2200 mm MAP. Geographic coordinates of each paired plot from the driest to wettest site are 40°15′S, 70°48′W; 39°57′S, 71°06′W; 40°26′S, 71°13′W; 40°04′S, 71°20′W, and 40°09′S, 71°34′W. The natural vegetation across the study sites varies from a shrub-grass steppe at the 250 and 650 mm MAP sites, to predominately *Nothofagus antarctica* woodlands and forests at the 1100 and 1350 mm MAP sites, to a mixed *N. dombeyi, N. nervosa,* and *N. obliqua* forest at the 2200 mm MAP site (Hess and Austin 2014, 2017).

Soils of the region formed from recently deposited layers of tephra over glacio-fluvial sediment. The oldest tephras in the region are about 10 kya, and the most recent (prior to our soil collection) deposits occurred in 1960 (Laya, 1977). The tephra is over 100 cm thick at the wettest site and thins moving east along the gradient. At the driest site, the glacio-fluvial sediments are buried by about 30 cm of tephra. Studies of pedogenesis across the site suggest that prior to the eruption of Puyehue-Cordón Caulle in 2011, the soil surface across the climate gradient derived from ash of the same eruption in 1960 (Colmet Daage et al., 1988; Ferrer et al., 1990).

Broquen et al. (2005) studied the development of andic properties in soils across a climosequence in close geographic proximity to that used for our study. As anticipated, the authors found young pedons with andic properties that increased in level of expression with rainfall. Ammonium oxalate extractable Fe, aluminum (Al), and silicon (Si), suggest that the amount of primary volcanic glass and short-range-order (SRO) Fe oxides in soils remain relatively constant across the rainfall gradient, but that the amount of allophane increases with precipitation, from 1 % to 10 % of the fine earth fraction (Broquen et al., 2005). These authors found that soil pH decreases with rainfall and that changes in pH were attributable to more exchangeable Al and OC in the high-rainfall sites. Ultimately, the soils were classified via the USDA Soil Taxonomy as Thaptic Udivitrands at 2000 mm MAP, Typic Hapludands at 1200 mm MAP, Humic Vitrixerands at 900 mm MAP, and Vitrandic Haploxerolls at 700 mm MAP (Broquen et al., 2005).

Extensive work has been done to characterize soils and ecosystem C and nitrogen (N) cycling across the precipitation gradient (Araujo, 2012; Hess and Austin, 2014; Araujo and Austin, 2015; Vivanco and Austin, 2019). These works demonstrated that pine afforestation significantly altered the C cycle in these ecosystems through multiple mechanisms. First, pines introduce shade at drier sites where decomposition is otherwise controlled by photodegradation (Austin and Vivanco, 2006; Austin et al., 2016), which results in slower litter decomposition rates in the pine plantations (Araujo and Austin, 2015). Second, pines increase total C stocks at the four driest sites by increasing live woody aboveground biomass and through the accumulation of recalcitrant pine litter on the forest floor (Araujo and Austin, 2020). On the other hand, pine afforestation was correlated with decreased soil organic C and N content along the gradient (Fig. S1), resulting in altered soil C:N ratios in the SOC pool (Hess and Austin, 2014). These patterns may be partly attributable to slower N turnover and lower microbial activity in the planted pine sites (Hess and Austin, 2017).

2.2. Soil sampling and extractions

We extracted air-dried soils originally collected by Hess and Austin (2014), wherein the sampling methodology is described at length. Soils were sampled at five random points along four transects every 10 m within a 50 x 50 m plot. The O horizon was removed, soils were sampled by push probe, and cores were separated into 0–5, 5–15, 15–30, 30–60, and 60–90 cm increments. At the two dry sites, due to difficulty in obtaining samples in the underlying glacio-fluvial sediment, 30–60 and 60–90 cm samples were not obtained. The five samples collected along each of the four transects were composited, so that five soil cores are incorporated into each sample, resulting in four composite soil profiles per site.

Soils samples were extracted using 0.5 M HCl in a 1:8 soil to HCl ratio, shaken for 24 h at room temperature (Heron et al., 1994; Teutsch et al., 1999; Wiederhold et al., 2007). After shaking, samples were filtered with Whatman 41 filter paper. Upon return to Pennsylvania State University, samples were additionally filtered with 0.45 uM polypropylene syringe filters prior to analysis on PerkinElmer Optima 7300 DV ICP-OES for a suite of geogenic metals: Al, Si, Fe, Ca, Mg, Na, K, P, and Mn.

The 0.5 M HCl extraction targets secondary amorphous mineral phases, especially Fe oxyhydroxides, and the exchangeable or adsorbed metals associated with those secondary amorphous phases (Chao and Zhou, 1983; Heron et al., 1994; Teutsch et al., 1999; Wiederhold et al., 2007; Yesavage et al., 2012). Recently, a similar dilute acid extraction has been demonstrated as necessary for full extraction of the plant available pools of Ca, K, and Mg that reside in organo-mineral complexes on secondary mineral phases (Bel et al., 2020). Over the course of pedogenesis, as primary minerals weather to form secondary minerals, the 24 hr 0.5 M HCl extraction extracts greater concentrations of metals until pedogenesis has proceeded such that SRO minerals crystallize. Past this point, as soils further weather, the extraction yields decreasing concentrations of the metals that comprise the majority of the SRO phases (Al, Fe, Si), but still extract the adsorbed, complexed, and exchangeable metal phases.

2.3. Statistical analysis

To assess the effect of MAP, MAT, and vegetation type on the extractable metal concentrations across the gradient, we used a multiple linear regression where vegetation type and MAP were the potential

explanatory variables of the concentrations of metals in soil extractions at each depth interval (R Core Team, 2017). Data satisfied the normality and homoscedasticity assumptions of linear regression.

Second, we calculated partial correlations of metal concentrations with ANPP (from Araujo and Austin, 2020) a at each depth interval, after controlling for vegetation type, MAP, and MAT. This test tells us how much variance is explained by ANPP after accounting for the variance explained by MAP, MAT, and vegetation type. We interpret significant correlation with ANPP to reflect biotic cycling of metals that cannot be explained by climate or vegetation type alone. Data were tested for and satisfied the assumptions of partial correlation analysis. Finally, to test the role of metals in explaining the SOC concentrations across the gradient, extractable metal concentration data were also incorporated into a model of SOC for each depth interval. Stepwise linear regression was conducted in SPSS version 28 (International Business Machines, Armonk, New York, United States). The criterion for model inclusion was $p < 0.02$, and the criterion for exclusion was $p < 0.05$. To limit collinearity, terms were further eliminated if the variable inflation factor (VIF) was greater than 3. Prior to the stepwise procedure, the following variables were included as possible explanatory variables of SOC: ANPP, MAP, MAT, vegetation type (planted pine or natural vegetation), and 0.5 M HCl extraction concentrations of Al, Si, Fe, Ca, Mg, Na, K, P, and Mn. Results from this model were compared to the multiple linear regression model of SOC in which only MAP and vegetation were included as explanatory variables (i.e., the model presented in Hess & Austin, 2014).

3. Results

3.1. Precipitation and vegetation significantly affect extracted cation concentrations

We found that extracted metal concentrations in the soil were significantly correlated with both vegetation type and MAP. To aid in the discussion of results from these multiple linear regressions, we sorted metal concentration response to vegetation and precipitation into two groups based on the metals' roles in soil minerals or plant nutrition. The first group (Fig. 2) represents extracted metal concentrations most often considered as constituents of soil minerals: Al, Si, Fe, Na, Mn. The second group (Fig. 3), represents metal concentrations of elements that are considered essential nutrients to plant growth: P, K, Ca, and Mg. Data from the 30–60 and 60–90 cm depth increments are reported in the supplementary information (Figures S2, S3).

Group 1 metals (Al, Si, Fe, Na, Mn) generally increase in concentration with MAP across the gradient (Figures 2, S2). In the 0–5, 5–15, and 15–30 cm increments Al concentration in metal extracts increased with increasing MAP ($p < 0.001$), but there was no significant effect of vegetation on the concentration of Al. The concentration of Si in the extracts increased with rainfall in the soil increments from 0 cm to 30 cm ($p < 0.05$), and the concentration of Si was higher in natural vegetation

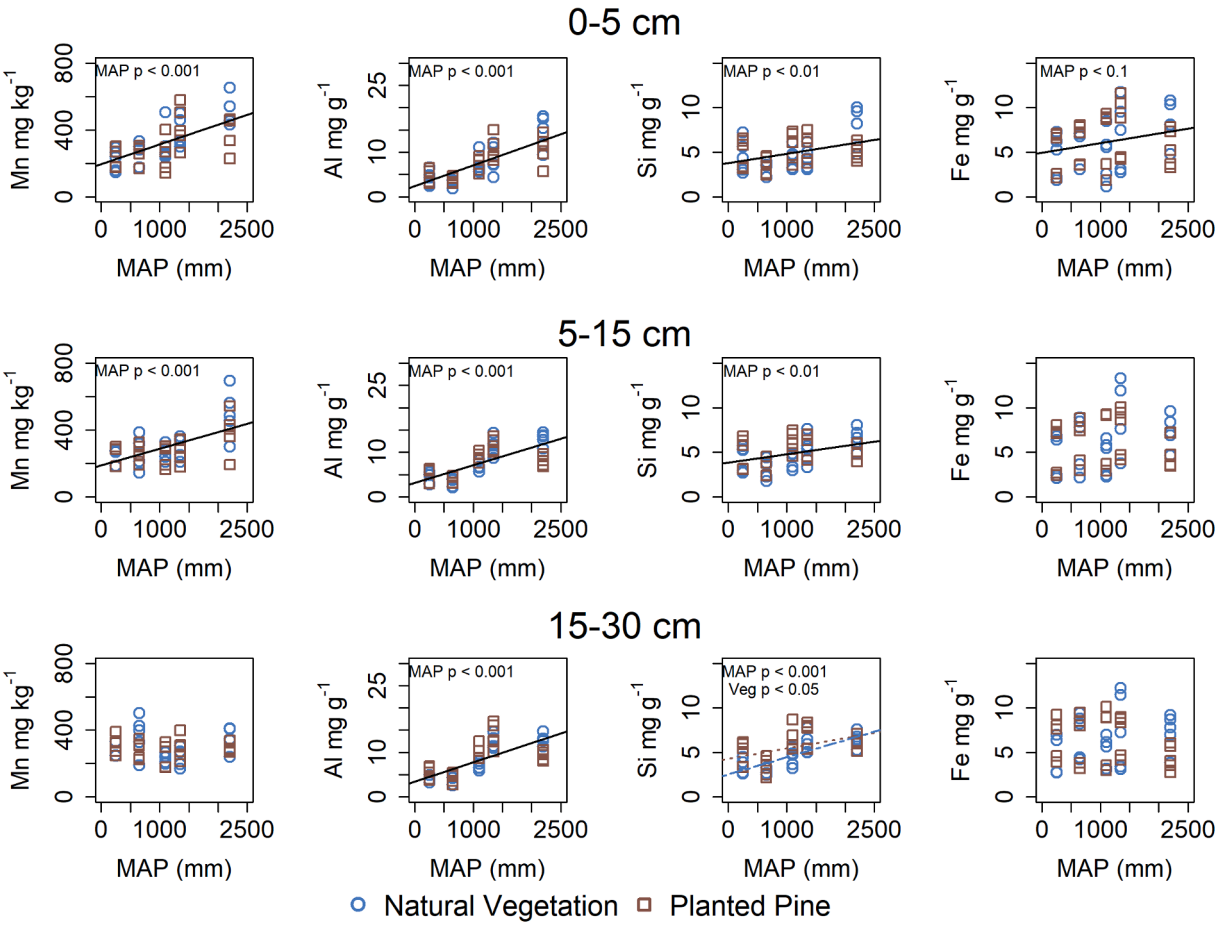

Fig. 2. Plots of extracted Mn, Al, Si, and Fe in the top 30 cm across the rainfall gradient. Blue circles represent the natural vegetation sites and brown squares represent planted pine sites. See supplementary information g the 30 – 60 and 60 – 90 depth increments (Figures S2). Significant regressions for MAP, vegetation, or the interaction between rainfall and vegetation are indicated with p-values on the individual plots. When only metal concentration is correlated with MAP, a solid black line represents the regression between the two variables. When both MAP and vegetation are significant factors, separate lines in dashed blue and dotted brown represent the regression for natural vegetation and planted pine, respectively. (For interpretation of the references to color in this figure legend, the reader is referred to the web version of this article.)

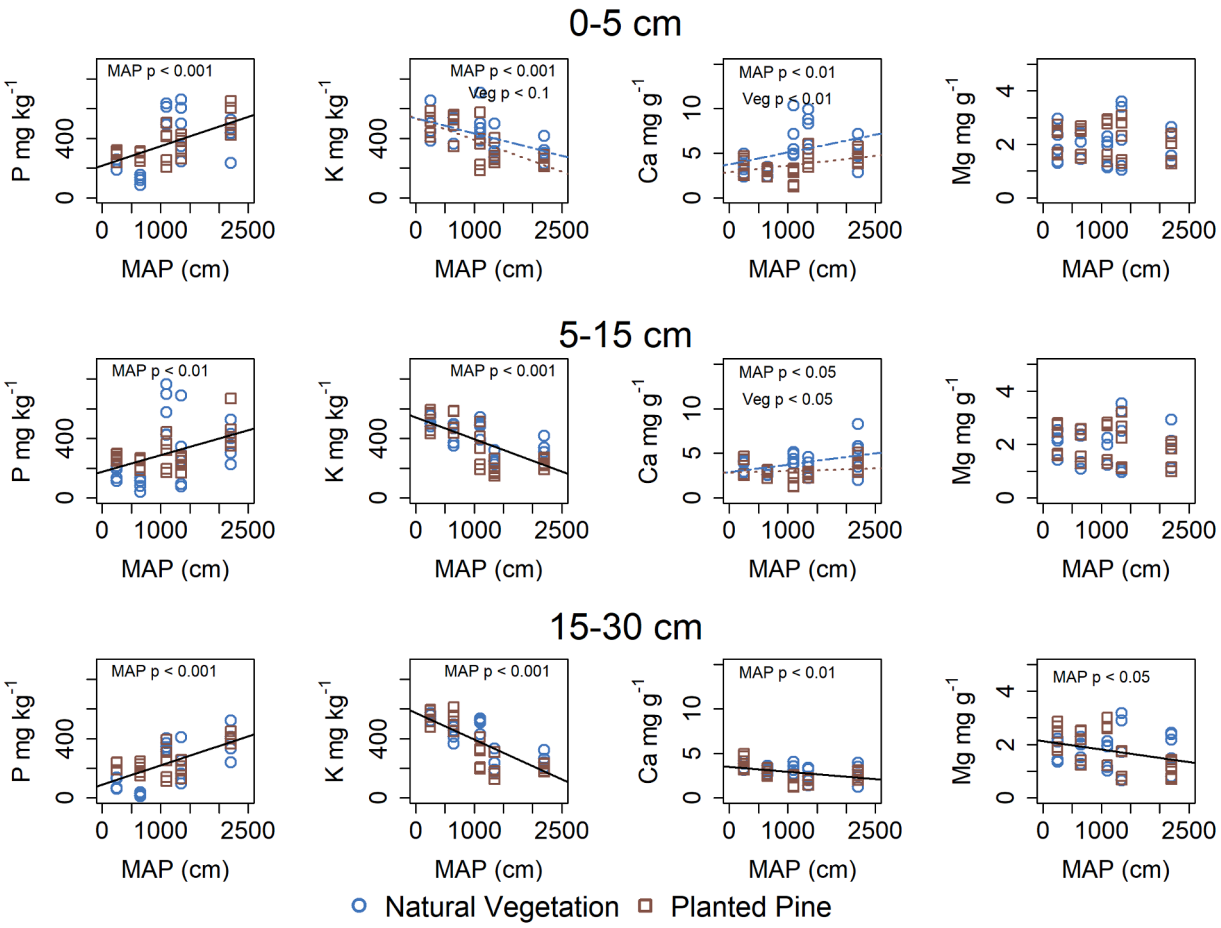

Fig. 3. Plots of extracted P, K, Ca, and Mg in the top 30 cm across the rainfall gradient. Blue circles represent the natural vegetation sites and brown squares represent planted pine sites. See supplementary information (Figures S3) for 30 – 60 and 60 – 90 depth increments. Significant regressions for MAP, vegetation, or the interaction between rainfall and vegetation are indicated with P-values on the individual plots. When only metal concentration correlated with MAP, a solid black line represents the regression between the two variables. When both MAP and vegetation are significant factors, separate lines in dashed blue and dotted brown represent the regression for natural vegetation and planted pine, respectively. (For interpretation of the references to color in this figure legend, the reader is referred to the web version of this article.)

sites at the 15–30 and 30–60 cm depth increments ($p < 0.05$). Fe significantly increased with rainfall in all depth increments from 0 to 30 cm, but not 30–90 cm; vegetation type did not significantly affect Fe concentration. The concentration of Na in extractions decreased with MAP in the 15–30 cm increment ($p < 0.1$), but the relationship between vegetation type or MAP was not significant at other depths. The concentration of Mn in the metal extracts increases with MAP in the 0–5, 5–15 cm ($p < 0.001$), and 30–60 cm ($p < 0.05$) increments, but there was no effect of vegetation type on Mn. In surface soils, no group 1 metals were correlated with MAT, but at 30–60 cm Si and Al were positively correlated with MAT ($p < 0.001$) and at 30–60 and 60–90 cm Si, Al, and Na were correlated with MAT (Figure S4). In general, all metals in group 1, aside from Na, increased in concentration with MAP, and few were significantly affected by vegetation type.

On the other hand, in group 2 (P, K, Ca, and Mg), each metal demonstrated idiosyncratic patterns with increasing MAP and afforestation (Fig. 3). The concentration of P in the extracts increased with MAP across all depth increments ($p < 0.05$). Additionally, at 15–30 cm the increase of P concentration with rainfall was less in afforested soils when compared to naturally vegetated sites (i.e., significant interaction of vegetation and precipitation, $p < 0.05$). The concentration of K decreased with MAP across all depth increments ($p < 0.05$), and soils with natural vegetation were higher in K concentration than afforested soils ($p < 0.1$). In the 0–5 and 5–15 cm, concentration of Ca increased significantly with MAP ($p < 0.05$) and was significantly higher in naturally vegetated sites ($p < 0.05$). In contrast, Ca decreased with MAP in the 15–30 cm increment. Finally, the concentration of Mg in extracts decreased with rainfall in the subsurface depths increments of 15–30, 30–60, and 60–90 cm.

Like the group 1 metals, no metal in group 2 was correlated with MAT in the top three depth increments. However, in the 30–60 and 60–90 cm increments, P, K, Ca, and Mg concentrations decreased as MAT increased ($p < 0.05$).

3.2. *Biotic activity weathers tephra regardless of climate or vegetation type*

We assessed how ANPP may influence soil metal concentrations across the climate gradient. We use this test as a measure of the role of plant activity over time, beyond what can be explained by MAP, MAT, and vegetation type alone, in weathering primary amorphous materials in the tephra parent material (Table 1). We found that ANPP, which is a measure of the yearly biomass increment of the vegetation, was a significant explanatory variable for Al, P, and Ca soil concentrations across all depth increments ($p < 0.05$) when controlling for MAP, MAT, and vegetation. We additionally found that ANPP significantly affected Mn at 60–90 cm ($p < 0.01$), K at 30–60 cm ($p < 0.05$), Si at 60–90 cm ($p < 0.05$) and Fe ($p < 0.05$) at 60–90 cm (Table 1).

Table 1
Partial correlation coefficients reflecting the effect of ANPP on extractable metal concentrations and C, after removing variance explained by vegetation, MAP, and MAT.

	0 – 5 cm		5 – 15 cm		15 – 30 cm		30 – 60 cm		60 – 90 cm	
	r	*p* Value	*r*	*p* Value	*r*	*p* Value	*r*	*p* Value	*r*	*p* Value
Mn	0.04	0.80	0.03	0.83	0.24	0.11	0.27	0.16	0.74	< 0.01***
Mg	−0.08	0.61	0.11	0.46	0.02	0.90	0.07	0.72	0.29	0.18
K	−0.19	0.21	−0.09	0.57	−0.24	0.11	−0.47	0.01**	0.04	0.87
Al	0.25	0.09*	0.30	0.04**	0.25	0.09*	0.42	0.03**	0.61	< 0.01***
Na	0.04	0.78	0.19	0.21	0.11	0.49	−0.01	0.97	0.35	0.11
Si	0.17	0.27	0.31	0.03	0.17	0.25	0.05	0.82	0.50	0.02**
P	−0.47	<0.01***	−0.51	< 0.01***	−0.40	< 0.01***	−0.67	< 0.01***	−0.48	0.02**
Ca	−0.43	< 0.01***	−0.27	0.08*	−0.35	0.02**	−0.59	<0.01***	−0.46	0.03**
Fe	0.13	0.38	0.18	0.22	0.11	0.47	0.16	0.41	0.46	0.03**
C	−0.15	0.31	−0.35	0.02**	−0.03	0.86	0.38	0.05*	0.21	0.34

*** $p < 0.01$; ** $p < 0.05$; * $p < 0.1$.

3.3. Inclusion of metalconcentrations improves model of SOC across sites

To test hypothesis 2, we included the soil metal concentrations, MAP, vegetation type, and ANPP into a stepwise linear regression model to compare with the simple (only MAP and vegetation type) model presented in Hess & Austin (2014). Inclusion of soil metal concentrations increased the explained variance in SOC concentrations by an average of 15 % across the depth intervals. Explained variance (adjusted R^2) increased from 52 % to 69 % at 0 – 5 cm; 75 % to 80 % at 5 – 15 cm; from 51 % to 73 % at 15 – 30 cm; from 14 % to 31 % at 30–60 cm; and from 0 % to 11 % at 60–90 cm.

In the new model, the best explanatory variables were different depending on soil depth. At 0–5 cm, both K ($p < 0.001$) and Ca ($p < 0.001$) were the best predictors, and the standardized coefficients demonstrated that SOC increased with Ca concentration, but decreased with increases in K. At 5–15 cm, MAP ($p < 0.001$), Al ($p < 0.001$), ANPP ($p < 0.001$), and Si ($p < 0.005$) were the best predictors of SOC; SOC increased with increases in MAP and Al concentrations but decreased with increases in ANPP and Si. At 15–30 cm, Al ($p < 0.001$), Na ($p < 0.001$), and vegetation type ($p < 0.01$) were significant predictors of SOC; the concentration of SOC increased with increases in Al but decreases with increases in Na and is lower in planted pine sites. At 30–60 cm, vegetation type ($p < 0.001$) and ANPP ($p < 0.01$) were better predictors than the vegetation and MAP of the original model. At this depth interval, SOC concentration decreased with increasing ANPP and was lower in planted pine sites. Finally, at 60–90 cm, only MAT ($p < 0.05$) was selected as a significant explanatory variable, and SOC concentration increased with increases in MAT.

To demonstrate the relationship between SOC and all potential explanatory variables, we also report the correlation coefficients for the multiple linear regression model with all potential explanatory variables included (Table 3), and the Spearman correlation coefficients of all potential explanatory variables with soil organic SOC (Table 4). Many of these terms were eliminated from the final model due to multicollinearity effects and to reduce VIF, even though they may be significantly correlated with SOC.

In the multiple linear regression model, aside from the explanatory variables included in the final models, SOC at 0–5 cm was positively correlated with MAP, Mn, and Al ($p < 0.01$) and SOC was significantly

Table 3
Correlation coefficients of variables for the final multiple linear regressions of potential explanatory variables for SOC concentration. Variables included in final model are bolded.

	0–5 cm	5–15 cm	15–30 cm	30–60 cm	60–90 cm
MAP	0.65***	**0.84*** **	0.69***	0.30	−0.01
MAT	−0.05	−0.23	−0.09	0.31*	**0.44****
ANPP	0.15	**0.35****	0.28*	**0.05**	−0.08
Mn	0.57***	0.52***	−0.11	0.14	0.09
Mg	−0.01	−0.11	−0.28**	−0.24	−0.23
K	**−0.38*** **	−0.63***	−0.73***	−0.25	−0.38*
Al	0.52***	**0.71*** **	**0.75*** **	0.27	0.33*
Na	−0.21	−0.24*	**−0.31****	−0.24	−0.06
Si	−0.14	**0.28***	0.51***	0.01	0.36*
Ca	**0.71*** **	0.35**	−0.44***	−0.07	−0.25
Fe	0.21	0.12	0.08	−0.03	−0.01
Vegetation	−0.36**	−0.22	**−0.26***	**−0.33***	−0.25

***$p < 0.01$; **$p < 0.05$; *$p < 0.1$.

Table 2
Multiple linear regression models of SOC using only rainfall and vegetation (Original Model, Hess and Austin, 2014) and then adding the metal extract concentrations, MAT, and ANPP as potential explanatory variables (New Model). Term inclusion was determined through stepwise step regression with a threshold of $p < 0.02$ for inclusion and $p < 0.05$ for exclusion. Further term exclusion was performed to ensure the variable inflation factor (VIF) for all explanatory variables < 3.

	Original Model				New Model			
	Term	Standardized Coefficient	*p* Value	Adj. R^2	Term	Standardized Coefficient	*p* Value	Adj. R^2
0 – 5 cm	MAP	0.64	< 0.001	0.52	K	−0.45	< 0.001	0.69
	Vegetation	−0.36	< 0.001		Ca	0.75	< 0.001	
5 – 15 cm	MAP	0.84	< 0.001	0.75	MAP	0.73	< 0.001	0.84
	Vegetation	−0.23	0.023		ANPP	−0.29	< 0.001	
					Al	0.64	< 0.001	
					Si	−0.37	0.001	
15 – 30 cm	MAP	0.68	< 0.001	0.51	Al	0.79	< 0.001	0.74
	Vegetation	−0.24	0.02		Na	−0.33	< 0.001	
					Veg	−0.23	0.005	
30 – 60 cm	MAP	0.30	0.07	0.14	Veg	−0.94	< 0.001	0.30
	Vegetation	−0.33	0.10		ANPP	−0.78	0.004	
60 – 90 cm	–		–	–	MAT	0.44	0.025	0.16

Table 4
Spearman correlation coefficients between extracted metal concentration, MAT, MAP, vegetation type, and ANPP with SOC concentration across sites.

	0–5 cm	5–15 cm	15–30 cm	30–60 cm	60–90 cm
MAP	0.89***	0.90***	0.83***	−0.37**	0.10
MAT	−0.17	−0.21	−0.04	0.28	0.44**
ANPP	0.36**	−0.37***	0.31**	0.04	−0.04
Mn	0.64***	0.49***	−0.09	0.10	0.16
Mg	−0.11	−0.18	−0.36**	−0.31*	−0.25
K	−0.50**	−0.61***	−0.76***	0.21	−0.43**
Al	0.70***	0.71***	0.73**	0.30	0.39**
Na	−0.20	−0.23	−0.31**	−0.26	−0.07
Si	0.22	0.26*	0.46***	0.08	0.41**
Ca	0.66***	0.22	−0.47***	−0.14	−0.36*
Fe	0.30**	0.14	0.01	−0.02	0.01
Vegetation	−0.29*	−0.23	−0.27*	−0.35*	−0.26

***$p < 0.01$; **$p < 0.05$; *$p < 0.1$.

lower in planted pine soils ($p < 0.05$). At 5–15 cm, SOC was positively correlated with Mn and Ca ($p < 0.01$) and was negatively correlated with Na ($p < 0.1$) and K ($p < 0.01$). For the 15–30 cm depth interval, Mg, Ca, and K ($p < 0.05$) were negatively correlated, and MAP, ANPP, and Si ($p < 0.1$) were positively correlated with SOC (Table 3). At 30–60 cm, only MAT was additionally correlated with SOC ($p < 0.1$). Finally, at 60–90 cm, K was negatively correlated, and Si was positively correlated with SOC at $p = 0.1$ (Table 3).

Table 4 demonstrates that SOC was correlated with many variables, even if not necessarily linear in relationship; here we highlight the most significant correlates of each depth increment. At 0–5 cm, the top three correlates with SOC were MAP, Mn, Al, and Ca, with Spearman correlation coefficients of 0.89, 0.64, 0.70, and 0.66, respectively ($p < 0.01$). In the 5–15 cm depth increment, the variables with the greatest correlation with SOC were MAP, Al, and K, at 0.90, 0.71, and −0.61 respectively ($p < 0.01$). In the 15–30 cm depth increment, the best correlates with SOC were MAP and K and they have correlation coefficients of 0.83 and −0.76 ($p < 0.01$). At 30–60 cm, MAP was the best correlate with SOC and has a correlation coefficient of −0.37 ($p < 0.01$). In the 60–90 cm depth increment, MAT, K, Al, Si, and Ca were all correlated with SOC ($p < 0.05$), with correlation coefficients of 0.44, −0.43, 0.39, 0.41, and −0.36.

4. Discussion

Our results demonstrate that 35 years of afforestation alters primary amorphous parent materials and the relationships between soil chemical properties and SOC concentrations in terrestrial ecosystems along a broad precipitation gradient. The increase in extractable Al, Fe, and Si concentrations in surface soils along the precipitation gradient in Patagonia signifies the weathering of primary minerals within tephra to form SRO aluminosilicates and Fe oxides. These minerals enhance the retention of nutrient cations, including P and Ca, which are actively cycled by vegetation. As expected across a climatic weathering gradient, concentrations of extractable base cations, especially monovalent ions, decreased with rainfall (Porder and Chadwick, 2009). These declines were more pronounced in planted pine soils, particularly of K throughout the soil profile and Ca in the subsurface. These patterns provide support for our first hypothesis, that lower base cation concentrations in soils are associated with conifers in contrast to broadleaf woody and herbaceous vegetation (Jobbágy and Jackson, 2003).

In support of our second hypothesis, the inclusion of extractable metal concentrations markedly improved the model of SOC along the precipitation gradient (Table 2). In addition, the highest correlates of SOC across depths were more often with the metal extract concentrations than MAP, MAT, or vegetation type. The positive correlation of SOC with Ca, Al, and Si across multiple depths suggests both direct sorption of SOC on secondary amorphous aluminosilicates and cation bridging by Ca contribute to the retention of SOC. As demonstrated in other volcanic soils (e.g., Matus et al., 2006, Panchini et al. 2017), Al complexation is likely increasingly important to SOC stabilization as MAP increases. The lower concentrations of Ca in afforested sites suggests that land conversion to planted pine may reduce the soil's capacity for SOC storage through cation bridging, an underappreciated consequence that should be considered in a more comprehensive evaluation of future afforestation efforts in the region and elsewhere.

4.1. Soil metals demonstrate weathering of primary minerals in volcanic ash

With increasing MAP, we observed increased concentrations of extractable Al, Si, P, Mn, and Fe in soil. This pattern likely represents weathering of primary amorphous glass to secondary Fe, Al, and Si-bearing SRO minerals with increasing rainfall, and retention of nutrients, like P and Mn on those secondary minerals. Broquen et al. (2005) demonstrated that allophane (a secondary SRO silicate) development increased with increasing precipitation in the soils of our study region; our results support this finding as both Al and Si concentrations increase in our extracts, but the rate of Al increase was greater than that of Si. The shift of Al:Si ratio from 1:1 to that of 2:1 in our extracts signals the formation of secondary SRO clay minerals like allophane (Parfitt et al., 1983; Parfitt and Childs, 1988; Dahlgren and Ugolini, 1989; Ugolini and Dahlgren, 2002).

Furthermore, the increase in extractable Fe with increasing MAP indicates the formation of SRO Fe oxyhydroxides, like ferrihydrite, which are known to increase in concentration with precipitation in young soils formed from volcanic materials (Chadwick et al., 2003; Dahlgren et al., 2004; Tsai et al., 2010). For example, Tsai et al. (2010) found that tephra-derived soils in a sub-tropical climate developed ferrihydrite and other SRO minerals as a function of increasing rainfall, while more crystalline secondary minerals developed in soils that received less precipitation. This pattern observed by Tsai et al. (2010) is similar to that observed at our sites, given the shifts in extractable Al, Si, and Fe with increasing rainfall. With further weathering, we would expect to observe more crystalline phases of metal oxides and aluminosilicates, at which point HCl-extractable metal concentrations might decrease. Thus, the increase in metals at the wettest sites of the gradient reflects that we captured a window in soil development when secondary SRO minerals are increasingly important. With time, these young tephra soils should shift to have fewer SRO minerals and extractable metals.

While not significantly correlated with metal extract concentrations or SOC in the top 30 cm of the soil profiles, MAT was significantly correlated with many metals in the 30–60 and 60–90 cm depth increments, and was the only factor selected in the stepwise regression of SOC at 60–90 cm (Table 2; Figures S4 and S5). These two depth increments only include samples from the three wettest sites (1100, 1350, and 2200 mm MAP), as the augerable depth only extended to 30 cm at 250 and 650 mm MAP. The temperature dependence of silicate weathering in sites with ample supply of weatherable minerals is well-established (Lebedeva et al., 2010; Dere et al., 2013; Li et al., 2016; Brantley et al., 2023), and research suggests that once soils reach a moisture threshold, temperature is the most important control on silicate weathering in many watersheds (Shaughnessy and Brantley, 2023). Considering that MAT is strongly positively correlated with Si and Al and negatively correlated with Na at 60–90 cm, and that Si and Al are also correlated with SOC at the 60–90 cm increment, the significance of MAT in the final model of SOC likely reflects the importance of MAT in driving weathering, the formation of secondary SRO minerals, and therefore SOC stabilization at the three wettest sites.

4.2. The role of biota in weathering volcanic glass and cycling base cations

Surprisingly, when controlling for variance explained by MAP, MAT, and vegetation type, ANPP is a significant explanatory factor for the

concentrations of Ca, Al, and P at all depth increments. This result suggests that the activity of plants is a key driver of the differences in element concentrations in soils across the gradient; for example, there is a clear signal of nutrient uplift in the depth profile of Ca, as the concentration of Ca in the 15–30 cm depth increment decreased with MAP, while in the 0–5 cm increment Ca concentration increased. Similarly, as ANPP increased, there was more P associated with the SRO minerals in soil at 0–5 cm depth than in the 15–30 cm increments. These patterns of nutrient uplift where biota draw nutrients from the subsurface to be tightly cycled in the surface soils, are well-established across ecosystems (Jobbágy and Jackson, 2004; Uhlig et al., 2017) and particularly in tropical soils derived from volcanic materials (Porder et al., 2007; Porder and Chadwick, 2009). Our data provide a temperate complement to these prior findings in tropical ecosystems.

The significant relationship between ANPP and Ca concentrations in the extracts, and the significantly lower Ca concentrations in the afforested soils, reflects a strong footprint of the biotic cycling of Ca in the soils across the study sites. Calcium is an essential nutrient and is a key component of structure, signaling and ion balance in terrestrial plants (White and Broadley, 2003). We propose that lower Ca concentrations in afforested soils results from the accumulation of undecomposed pine needles and woody biomass on the soil surface (Araujo and Austin, 2020). This thick, slowly decomposing litter layer locks up Ca in organic forms not available for plant uptake, which may result in afforested rhizospheres that are depleted in Ca. On the other hand, a thick litter layer is not present at the naturally vegetated sites (Araujo and Austin, 2020), and decomposition rates are generally faster. As such, in the sites of natural vegetation, base nutrients within plant litter, like Ca, may be more efficiently recycled and returned to soils, which is reflected in the soil Ca concentrations in this study.

The shift in base cation pools from soils to biomass in afforested sites is well-supported in the literature. Richter et al. (1994) reported that 30 years of afforestation in kaolinite-rich Ultisols resulted in redistribution of base cations, especially Ca and Mg, from soils to woody biomass and leaf litter. Similarly, in the Pampas of Argentina, Jobbágy and Jackson (2003) demonstrated that afforestation of the native grassland resulted in lower Ca, Mg, and Mn in the mineral soil because the trees stored these base cations in slow to recycle woody biomass. Further, in the high-altitude tropical Andes of Ecuador, mass loss of base cations from soils of forested sites was found to be nearly 20 % higher than in adjacent grasslands (Molina et al., 2019). All of these findings agree with a *meta*-analysis of afforested soils which reports that pine afforestation significantly reduces the concentration of K by 23 % and Ca by 31 % compared to naturally vegetated sites (Berthrong et al., 2009).

4.3. Revised model of SOC demonstrates the importance of metal complexes and cation bridging

The results of the multiple linear regression models demonstrate that mineral stabilization of SOC may be a significant contributor to the increase of organic C concentrations in the soils across the rainfall gradient, and that results of a relatively simple extraction protocol can illuminate mechanisms of soil C retention in soils. Importantly, the new models (Table 2) that included the metal extract concentrations increased the explained variance in SOC concentrations across all depth increments.

The inclusion of Al concentrations in the final multiple linear regression model (Table 2) and the significant positive correlation between SOC and Al (Tables 3 and 4) points to the importance of Al-organic matter complexes in the stabilization of SOC in the soils of our study sites. Furthermore, the influence of ANPP in explaining the soil concentrations of Al suggests the importance of organic complexes with Al to soil C storage as plant growth and aboveground biomass increase. Broquen et al. (2005) found that soils of the region increase in Al-organic matter complexes with increasing precipitation, and a study of 225 pedons demonstrated that Al is the main factor controlling SOC stocks in volcanic soils across Chile (Matus et al., 2006). Aluminum complexation was established as a the key mechanism of soil C retention across these Chilean Andisols (Garrido and Matus, 2012). Furthermore, previous work demonstrated that Al-organic matter complexes act as a significant mechanism of C stabilization in volcanic soils that develop in a tropical climate (Masiello et al., 2004).

Our results strongly suggest that Al complexes with organic matter may also be key to C stabilization in volcanic soils of humid temperate climates within Patagonia. However, the mechanisms behind the stabilization of organic matter through complexation with Al are not well-constrained. Some potential stabilization mechanisms include cation bridging to form stable organo-Al-mineral complexes, coagulation of associated organic matter that renders organic functional groups less accessible to enzymatic attack, and promotion of aggregation at the micro and macroaggregate scales (Takahashi and Dahlgren, 2016).

The multiple linear regression model also demonstrated that lower Ca concentrations in afforested soils affected the SOC storage potential across the rainfall gradient. The importance of Ca in stabilizing SOC via cation bridging with aluminosilicates (Muneer and Oades, 1989; Wattel-Koekkoek et al., 2001; Sutton and Sposito, 2006) and Al and Fe oxyhydroxides (Rasmussen et al., 2005; Sowers et al., 2018a) is well-established. Indeed, recent works report that soil Ca extracts are one of the best predictors of SOC across landscapes (Rasmussen et al., 2018; Wang et al., 2021). In our afforested sites of the Patagonian Andes, the redistribution of Ca from soil cation exchange sites to plant biomass likely reduced the potential for cation bridging as a SOC stabilization mechanism.

4.4. Implications

We used results of a simple soil extraction protocol to significantly improve a model of SOC across a climate gradient with natural vegetation and pine afforestation paired plots in young tephra-derived soils. The significance of these metal extracts to SOC stocks in soils reflects plant species composition and precipitation are important factors governing SOC accumulation in soils, but that mineralogical controls on C stabilization may also play a fundamental role (Doetterl et al., 2015). While our extractions cannot provide confirmation of the mechanisms of soil C storage, the significance of Al and Ca in the model, and the results of previous studies (Broquen et al., 2005; Hobbie et al., 2007; Matus et al., 2006; Percival et al., 2000; Rasmussen et al., 2018; Wang et al., 2021), suggest that both cation bridging with Ca and complexation with Al may be important in stabilizing C in the soils of the Patagonian Andes. Importantly, while previous studies of tephra-derived soils have established mechanisms of SOC storage, many of those studies were based in tropical and sub-tropical climates (e.g., Schuur et al., 2001; Masiello et al., 2004; Gamboa and Galicia, 2012; Kramer and Chadwick, 2016). Our study builds upon the previous works on soil C storage in temperate, volcanic-derived soils (e.g., Broquen et al., 2005; Garrido and Matus, 2012; Matus et al., 2006; Panichini et al., 2017) derived from tephra by probing soil C storage across a rainfall gradient of different vegetation types.

Our results also suggest that along this regional precipitation gradient in Patagonia, pine afforestation decreases SOC stocks by decreasing base cation concentrations and the potential for Ca bridging in these young tephra-derived soils. Although a global *meta*-analysis of studies demonstrated that afforestation has a net neutral to net positive effect on SOC stocks (Li et al., 2012), our findings present previously unforeseen impacts of afforestation projects. When afforesting with conifers in former grasslands and shrublands, there is a potential for redistribution of Ca and other cations from exchange sites to plant biomass. When stored in biomass and plant litter, these base cations cannot aid in soil C stabilization through aggregation and cation bridging. These relationships between base cations and SOC in afforested sites may help explain further shifts in SOC stocks under anthropogenic climate and land use change. The loss of soil C storage capacity

at the expense of rapidly growing above ground vegetation should be weighed carefully.

Declaration of Competing Interest

The authors declare that they have no known competing financial interests or personal relationships that could have appeared to influence the work reported in this paper.

Data availability

Data will be made available on request.

Acknowledgement

Financial Support was provided by United States Department of Agriculture, National Institute of Food and Agriculture Grant #2020-67034-31716 and a National Science Foundation Science Across Virtual Institutes Scholarship to CH. The authors thank Luis Ignacio Perez for field and laboratory assistance. We also thank two anonymous reviewers who provided suggestions that significantly improved our manuscript.

Statements and Declarations.

USDA NIFA #2020-67034-31716 to CH, and NSF CZO SAVI scholarship to CH for travel to Argentina and analytical costs associated with the study.

Appendix A. Supplementary data

Supplementary data to this article can be found online at https://doi.org/10.1016/j.geoderma.2023.116718.

References

Amundson, R., 2001. The Carbon Budget in Soils. Annu Rev Earth Pl Sc 29, 535–562. https://doi.org/10.1146/annurev.earth.29.1.535.

Araujo, P.I., 2012. Impactos de las plantaciones de pino sobre el ciclo de carbono a lo largo de un gradiente de precipitaciones en la Patagonia, Argentina. IFEVA-Facultad de Agronomía. Universidad de Buenos Aires. Graduate Thesis.

Araujo, P.I., Austin, A.T., 2015. A shady business: pine afforestation alters the primary controls on litter decomposition along a precipitation gradient in Patagonia, Argentina. J Ecol 103, 1408–1420. https://doi.org/10.1111/1365-2745.12433.

Araujo, P.I., Austin, A.T., 2020. Exotic pine forestation shifts carbon accumulation to litter detritus and wood along a broad precipitation gradient in Patagonia. Argentina. Forest Ecol Manag 460, 117902. https://doi.org/10.1016/j.foreco.2020.117902.

Austin, A.T., Méndez, M.S., Ballaré, C.L., 2016. Photodegradation alleviates the lignin bottleneck for carbon turnover in terrestrial ecosystems. Proc National Acad Sci 113, 4392–4397. https://doi.org/10.1073/pnas.1516157113.

Austin, A.T., Vivanco, L., 2006. Plant litter decomposition in a semi-arid ecosystem controlled by photodegradation. Nature 442, 555–558. https://doi.org/10.1038/nature05038.

Bel, J., Legout, A., Saint-André, L., Hall, S.J., Löfgren, S., Laclau, J.P., van der Heijden, G., 2020. Conventional analysis methods underestimate the plant-available pools of calcium, magnesium and potassium in forest soils. Scientific Reports 10 (1), 15703.

Berthrong, S.T., Jobbágy, E.G., Jackson, R.B., 2009. A global meta-analysis of soil exchangeable cations, pH, carbon, and nitrogen with afforestation. Ecol Appl 19, 2228–2241. https://doi.org/10.1890/08-1730.1.

Blankinship, J.C., Berhe, A.A., Crow, S.E., et al., 2018. Improving understanding of soil organic matter dynamics by triangulating theories, measurements, and models. Biogeochemistry 140, 1–13. https://doi.org/10.1007/s10533-018-0478-2.

Brantley, S.L., Shaughnessy, A., Lebedeva, M.I., Balashov, V.N., 2023. How temperature-dependent silicate weathering acts as Earth's geological thermostat. Science 379 (6630), 382–389. https://doi.org/10.1126/science.add2922.

Broquen, P., Lobartini, J.C., Candan, F., Falbo, G., 2005. Allophane, aluminum, and organic matter accumulation across a bioclimatic sequence of volcanic ash soils of Argentina. Geoderma 129, 167–177. https://doi.org/10.1016/j.geoderma.2004.12.041.

Chadwick, O.A., Gavenda, R.T., Kelly, E.F., et al., 2003. The impact of climate on the biogeochemical functioning of volcanic soils. Chemical Geology 202, 195–223. https://doi.org/10.1016/j.chemgeo.2002.09.001.

Chao, T.T., Zhou, L., 1983. Extraction Techniques for Selective Dissolution of Amorphous Iron Oxides from Soils and Sediments. Soil Sci Soc Am J 47, 225–232. https://doi.org/10.2136/sssaj1983.03615995004700020010x.

Chorover, J., Amistadi, M., Chadwick, O., 2004. Surface charge evolution of mineral-organic complexes during pedogenesis in Hawaiian basalt. Geochimica Et Cosmochimica Acta 68. https://doi.org/10.1016/j.gca.2004.06.005.

Colmet Daage, F., Marcolin, A., López, C., Lanciotti, M., Ayesa, J., Bran, D., Bouleau, P., 1988. Características de los suelos derivados de cenizas volcánicas de la cordillera y precordillera del norte de la Patagonia. Bariloche. Convenio INTA-ORSTOM, SC de Bariloche, Río Negro.

Dahlgren, R.A., Saigusa, M., Ugolini, F.C., 2004. The Nature, Properties and Management of Volcanic Soils. Advances in Agronomy 82, 113–182. https://doi.org/10.1016/s0065-2113(03)82003-5.

Dahlgren, R.A., Ugolini, F.C., 1989. Formation and stability of imogolite in a tephritic Spodosol, Cascade Range, Washington, USA. Geochimica Et Cosmochimica Acta 53 (8), 1897–1904.

Dere, A.L., White, T.S., April, R.H., Reynolds, B., Miller, T.E., Knapp, E.P., McKay, L.D., Brantley, S.L., 2013. Climate dependence of feldspar weathering in shale soils along a latitudinal gradient. Geochimica Et Cosmochimica Acta 122, 101–126. https://doi.org/10.1016/j.gca.2013.08.001.

Doetterl, S., Stevens, A., Six, J., et al., 2015. Soil carbon storage controlled by interactions between geochemistry and climate. Nat Geosci 8, 780–783. https://doi.org/10.1038/ngeo2516.

Ferrer, J., Irisarri, J., & Mendía, M. (1990). Síntesis de los factores del medio geográfico y de las propiedades de los suelos. *CFI-COPADE-Prov. NQN (eds.) Estudio Regional de Suelos de la Provincia del Neuquén*, *1*.

Gamboa, A.M., Galicia, L., 2012. Land-use/cover change effects and carbon controls on volcanic soil profiles in highland temperate forests. Geoderma 170, 390–402. https://doi.org/10.1016/j.geoderma.2011.11.021.

Garrido, E., Matus, F., 2012. Are organo-mineral complexes and allophane content determinant factors for the carbon level in Chilean volcanic soils? Catena 92, 106–112. https://doi.org/10.1016/j.catena.2011.12.003.

Harden, J.W., Hugelius, G., Ahlström, A., et al., 2018. Networking our science to characterize the state, vulnerabilities, and management opportunities of soil organic matter. Global Change Biol 24, e705–e718. https://doi.org/10.1111/gcb.13896.

Heron, G., Crouzet, C., Bourg, A.C.M., Christensen, T.H., 1994. Speciation of Fe(II) and Fe(III) in Contaminated Aquifer Sediments Using Chemical Extraction Techniques. Environmental Science & Technology 28 (9), 1698–1705. https://doi.org/10.1021/es00058a023.

Hess, L.J.T., Austin, A.T., 2014. Pinus ponderosa alters nitrogen dynamics and diminishes the climate footprint in natural ecosystems of Patagonia. J Ecol 102, 610–621. https://doi.org/10.1111/1365-2745.12228.

Hess, L.J.T., Austin, A.T., 2017. Pine afforestation alters rhizosphere effects and soil nutrient turnover across a precipitation gradient in Patagonia, Argentina. Plant Soil 415, 449–464. https://doi.org/10.1007/s11104-017-3174-4.

Hobbie, S.E., Ogdahl, M., Chorover, J., et al., 2007. Tree Species Effects on Soil Organic Matter Dynamics: The Role of Soil Cation Composition. Ecosystems 10, 999–1018. https://doi.org/10.1007/s10021-007-9073-4.

Jandl, R., Lindner, M., Vesterdal, L., Bauwens, B., Baritz, R., Hagedorn, F., Johnson, D. W., Minkkinen, K., Byrne, K.A., 2007. How strongly can forest management influence soil carbon sequestration? Geoderma 137 (3–4), 253–268. https://doi.org/10.1016/j.geoderma.2006.09.003.

Jobbágy, E.G., Jackson, R.B., 2003. Patterns and mechanisms of soil acidification in the conversion of grasslands to forests. Biogeochemistry 64 (2), 205–229. https://doi.org/10.1023/a:1024985629259.

Jobbágy, E.G., Jackson, R.B., 2004. The uplift of soil nutrients by plants: biogeochemical consequences across scales. Ecology 85, 2380–2389. https://doi.org/10.1890/03-0245.

Kleber, M., Eusterhues, K., Keiluweit, M., et al., 2015. Advances in Agronomy. 130, 1–140. https://doi.org/10.1016/bs.agron.2014.10.005.

Kramer, M.G., Chadwick, O.A., 2016. Controls on carbon storage and weathering in volcanic soils across a high-elevation climate gradient on Mauna Kea. Hawaii. Ecology 97, 2384–2395. https://doi.org/10.1002/ecy.1467.

Lawrence, C.R., Schulz, M.S., Masiello, C.A., et al., 2021. The trajectory of soil development and its relationship to soil carbon dynamics. Geoderma 403, 115378. https://doi.org/10.1016/j.geoderma.2021.115378.

Laya, H., 1977. Edafogenesis y paleosuelos de la formacion tefrica rio pireco (Holoceno). Suroeste de la provencia del Neuquen. Argentina. as Geol Argent. 32, 2–23.

Lebedeva, M.I., Fletcher, R.C., Brantley, S.L., 2010. A mathematical model for steady-state regolith production at constant erosion rate. Earth Surface Processes and Landforms 35 (5), 508–524. https://doi.org/10.1002/esp.1954.

Li, G., Hartmann, J., Derry, L.A., West, A.J., You, C.-F., Long, X., Zhan, T., Li, L., Li, G., Qiu, W., Li, T., Liu, L., Chen, Y., Ji, J., Zhao, L., Chen, J., 2016. Temperature dependence of basalt weathering. Earth and Planetary Science Letters 443, 59–69. https://doi.org/10.1016/j.epsl.2016.03.015.

Li, D., Niu, S., Luo, Y., 2012. Global patterns of the dynamics of soil carbon and nitrogen stocks following afforestation: a meta-analysis. New Phytol 195, 172–181. https://doi.org/10.1111/j.1469-8137.2012.04150.x.

Masiello, C., Chadwick, O., Southon, J., 2004. Weathering controls on mechanisms of carbon storage in grassland soils. Global Biogeochemical Cycles 18. https://doi.org/10.1029/2004GB002219.

Mathieu, J.A., Hatté, C., Balesdent, J., Parent, É., 2015. Deep soil carbon dynamics are driven more by soil type than by climate: a worldwide meta-analysis of radiocarbon profiles. Glob Change Biol 21, 4278–4292. https://doi.org/10.1111/gcb.13012.

Matus, F., Amigo, X., Kristiansen, S.M., 2006. Aluminium stabilization controls organic carbon levels in Chilean volcanic soils. Geoderma 132, 158–168. https://doi.org/10.1016/j.geoderma.2005.05.005.

Matus, F., Rumpel, C., Neculman, R., et al., 2014. Soil carbon storage and stabilisation in andic soils: A review. Catena 120, 102–110. https://doi.org/10.1016/j.catena.2014.04.008.

Mikutta, R., Kleber, M., Torn, M.S., Jahn, R., 2006. Stabilization of Soil Organic Matter: Association with Minerals or Chemical Recalcitrance? Biogeochemistry 77, 25–56. https://doi.org/10.1007/s10533-005-0712-6.

Mikutta, R., Schaumann, G.E., Gildemeister, D., Bonneville, S., Kramer, M.G., Chorover, J., Guggenberger, G., 2009. Biogeochemistry of mineral–organic associations across a long-term mineralogical soil gradient (0.3–4100 kyr), Hawaiian Islands. Geochimica Et Cosmochimica Acta 73 (7), 2034–2060.

Molina, A., Vanacker, V., Corre, M.D., Veldkamp, E., 2019. Patterns in Soil Chemical Weathering Related to Topographic Gradients and Vegetation Structure in a High Andean Tropical Ecosystem. J Geophys Res Earth Surf 124, 666–685. https://doi.org/10.1029/2018jf004856.

Muneer, M., Oades, J., 1989. The role of Ca-organic interactions in soil aggregate stability.III. Mechanisms and Models. Soil Res 27, 411–423. https://doi.org/10.1071/sr9890411.

Nave, L.E., Domke, G.M., Hofmeister, K.L., Mishra, U., Perry, C.H., Walters, B.F., Swanston, C.W., 2018. Reforestation can sequester two petagrams of carbon in US topsoils in a century. Proceedings of the National Academy of Sciences 115 (11), 2776–2781. https://doi.org/10.1073/pnas.1719685115.

Panichini, M., Neculman, R., Godoy, R., Arancibia-Miranda, N., Matus, F., 2017. Understanding carbon storage in volcanic soils under selectively logged temperate rainforests. Geoderma 302, 76–88. https://doi.org/10.1016/j.geoderma.2017.04.023.

Parfitt, R., Childs, C., 1988. Estimation of forms of Fe and Al - a review, and analysis of contrasting soils by dissolution and Mossbauer methods. Soil Res 26, 121–144. https://doi.org/10.1071/sr9880121.

Parfitt, R.L., Russell, M., Orbell, G.E., 1983. Weathering sequence of soils from volcanic ash involving allophane and halloysite, New Zealand. Geoderma 29, 41–57. https://doi.org/10.1016/0016-7061(83)90029-0.

Percival, H.J., Parfitt, R.L., Scott, N.A., 2000. Factors Controlling Soil Carbon Levels in New Zealand Grasslands: Is Clay Content Important? Soil Science Society of America Journal 64 (5), 1623–1630. https://doi.org/10.2136/sssaj2000.6451623x.

Porder, S., Chadwick, O.A., 2009. Climate and soil age constraints on nutrient uplift and retention by plants. Ecology 90. https://doi.org/10.1890/07-1739.1.

Porder, S., Vitousek, P., Chadwick, O., Chamberlain, C., 2007. Uplift, erosion, and phosphorus limitation in terrestrial ecosystems. Ecosystems 10. https://doi.org/10.1007/s10021-006-9011-x.

R Core Team, 2017. R: A language and environment for statistical computing. R Foundation for Statistical Computing, Vienna, Austria https://www.R-project.org/.

Rasmussen, C., Torn, M.S., Southard, R.J., 2005. Mineral Assemblage and Aggregates Control Carbon Dynamics in a California Conifer Forest. Soil Sci Soc Am J 69, 1711–1721. https://doi.org/10.2136/sssaj2005.0040.

Rasmussen, C., Heckman, K., Wieder, W.R., et al., 2018. Beyond clay: towards an improved set of variables for predicting soil organic matter content. Biogeochemistry 137, 297–306. https://doi.org/10.1007/s10533-018-0424-3.

Richter, D.D., Markewitz, D., Wells, C.G., Allen, H.L., April, R., Heine, P.R., Urrego, B., 1994. Soil Chemical Change during Three Decades in an Old-Field Loblolly Pine (Pinus Taeda L.). Ecosystem. Ecology 75 (5), 1463–1473. https://doi.org/10.2307/1937469.

Rowley, M.C., Grand, S., Verrecchia, É.P., 2018. Calcium-mediated stabilisation of soil organic carbon. Biogeochemistry 137, 27–49. https://doi.org/10.1007/s10533-017-0410-1.

Schuur, E., Chadwick, O., Matson, P., 2001. Carbon cycling and soil carbon storage in mesic to wet Hawaiian montane forests. Ecology 82. https://doi.org/10.1890/0012-9658(2001)082[3182:CCASCS]2.0.CO;2.

Shaughnessy, A.R., Brantley, S.L., 2023. How do silicate weathering rates in shales respond to climate and erosion? Chemical Geology 629, 121474. https://doi.org/10.1016/j.chemgeo.2023.121474.

Sowers, T.D., Adhikari, D., Wang, J., et al., 2018a. Spatial Associations and Chemical Composition of Organic Carbon Sequestered in Fe, Ca, and Organic Carbon Ternary Systems. Environ Sci Technol 52, 6936–6944. https://doi.org/10.1021/acs.est.8b01158.

Sowers, T.D., Stuckey, J.W., Sparks, D.L., 2018b. The synergistic effect of calcium on organic carbon sequestration to ferrihydrite. Geochem T 19, 4. https://doi.org/10.1186/s12932-018-0049-4.

Sutton, R., Sposito, G., 2006. Molecular simulation of humic substance–Ca-montmorillonite complexes. Geochim Cosmochim Ac 70, 3566–3581. https://doi.org/10.1016/j.gca.2006.04.032.

Takahashi, T., Dahlgren, R.A., 2016. Nature, properties and function of aluminum–humus complexes in volcanic soils. Geoderma 263, 110–121. https://doi.org/10.1016/j.geoderma.2015.08.032.

Teutsch, N., Erel, Y., Halicz, L., Chadwick, O.A., 1999. The influence of rainfall on metal concentration and behavior in the soil. Geochim Cosmochim Ac 63, 3499–3511. https://doi.org/10.1016/s0016-7037(99)00152-0.

Tsai, C.C., Chen, Z.S., Kao, C.I., et al., 2010. Pedogenic development of volcanic ash soils along a climosequence in Northern Taiwan. Geoderma 156, 48–59. https://doi.org/10.1016/j.geoderma.2010.01.007.

Ugolini, F.C., Dahlgren, R.A., 2002. Soil Development in Volcanic Ash. Global Environmental Research 6 (2), 69–81.

Uhlig, D., Schuessler, J.A., Bouchez, J., et al., 2017. Quantifying nutrient uptake as driver of rock weathering in forest ecosystems by magnesium stable isotopes. Biogeosciences 14, 3111–3128. https://doi.org/10.5194/bg-14-3111-2017.

Uhlig, D., Amelung, W., Von Blanckenburg, F., 2020. Mineral nutrients sourced in deep regolith sustain long-term nutrition of mountainous temperate forest ecosystems. Global Biogeochemical Cycles 34 (9), e2019G–B006513.

Vivanco, L., Austin, A.T., 2019. The importance of macro- and micro-nutrients over climate for leaf litter decomposition and nutrient release in Patagonian temperate forests. Forest Ecol Manag 441, 144–154. https://doi.org/10.1016/j.foreco.2019.03.019.

Wang, C., Sun, Y., Chen, H.Y.H., et al., 2021. Meta-analysis shows non-uniform responses of above- and belowground productivity to drought. Sci Total Environ 782, 146901. https://doi.org/10.1016/j.scitotenv.2021.146901.

Wattel-Koekkoek, E.J.W., van Genuchten, P.P.L., Buurman, P., van Lagen, B., 2001. Amount and composition of clay-associated soil organic matter in a range of kaolinitic and smectitic soils. Geoderma 99, 27–49. https://doi.org/10.1016/s0016-7061(00)00062-8.

White, P.J., Broadley, M.R., 2003. Calcium in Plants. Ann Bot-London 92, 487–511. https://doi.org/10.1093/aob/mcg164.

Wiederhold, J.G., Teutsch, N., Kraemer, S.M., Halliday, A.N., Kretzschmar, R., 2007. Iron isotope fractionation in oxic soils by mineral weathering and podzolization. Geochimica Et Cosmochimica Acta 71 (23), 5821–5833.

Yesavage, T., Fantle, M.S., Vervoort, J., et al., 2012. Fe cycling in the Shale Hills Critical Zone Observatory, Pennsylvania: An analysis of biogeochemical weathering and Fe isotope fractionation. Geochimica Et Cosmochimica Acta 99, 18–38.